In-depth insights into N_2O formation over Rh- and Pt-based LNT catalysts

L. Castoldi[a,*], R. Matarrese[a], L. Kubiak[a], M. Daturi[b], N. Artioli[b,1], S. Pompa[a], L. Lietti[a,*]

[a] *Politecnico di Milano, Laboratory of Catalysis and Catalytic Processes, Dipartimento di Energia, Via La Masa 34, 20156 Milano, Italy*
[b] *Normandie Université, ENSICAEN, CNRS, Laboratoire Catalyse et Spectrochimie, 14000 Caen, France*

ARTICLE INFO

ABSTRACT

In this paper mechanistic aspects involved in the formation of N_2O over model Pt-Ba/Al$_2$O$_3$ and Rh-Ba/Al$_2$O$_3$ LNT catalysts are discussed. The reactivity of both gaseous NO and of stored NO$_x$ (nitrates) has been studied, with simultaneous surface characterization by *operando* FT-IR spectroscopy, using different reductants (i.e. H$_2$, CO, CO + H$_2$, CO + H$_2$O) both under isothermal conditions and temperature programming. The results show that N_2O formation may occur during both the lean/rich and rich/lean switches (primary and secondary N_2O, respectively). In particular: i) primary N_2O formation involves the presence of gas-phase NO and partially reduced metal sites; ii) N_2O formation increases in the presence of CO because the reduction of the metal sites is slower, thus favoring N_2O formation upon the lean/rich transition; iii) residual reducing species onto the surface (i.e. NCO$^-$, CO) can react with NO giving the secondary N_2O peak. A reaction pathway for N_2O formation is suggested where metal sites (Pt or Rh) catalyse the NO dissociation reaction into N- and O-adatoms; N-species further interact with undissociated NO molecules leading to the formation of N_2O (primary N_2O). In additions, isocyanates formed during the NO$_x$ reduction in the presence of CO may participate in the N_2O formation upon reaction with NO during the lean phase (secondary N_2O).

Pt- and Rh-based catalysts show similar behavior even if Rh-based catalyst is less reactive than Pt-based sample likely due to the lower dispersion of the noble metal.

1. Introduction

In densely populated areas, traffic emissions are a significant source of pollutants. Some of them are short lived and have mainly local health and environmental effects; those include carbon black and NO$_x$. Long lived gases, like CO$_2$, CH$_4$, N$_2$O are greenhouse gases and have global effects on atmospheric chemistry and climate.

Catalytic elimination of environmental pollutants from passenger cars is a permanent challenge for researchers. Particularly, NO$_x$ reduction from exhaust gas of diesel and lean-burn engines is still a problem for car manufacturers. Among the processes effective to reduce NO$_x$ in lean condition, lean NO$_x$ traps (LNTs, also known as NO$_x$ Storage Reduction (NSR) catalysts) represent a viable technology either as a stand-alone system or complemented by an urea-SCR system. The LNT catalytic system, introduced by Toyota in '90, contains three fundamental components: a high surface area support like γ-Al$_2$O$_3$, a NO$_x$ absorber material like alkaline or alkaline-earth metal oxide (Ba, K) and noble metals such as Pt, Rh, Pd. Promoters and additives like Zr, Ce may be also included to increase thermal stability and add Oxygen Storage Capacity (OSC) functionality [1]. In NSR catalysts the NO$_x$ conversion is

achieved on the basis of cyclic operations alternating between lean (60–90 s) and rich (1–3 s) conditions: NO$_x$ are adsorbed on the catalyst surface during lean operations, while the trap is regenerated under the fuel rich environment [1–3]. Among the disadvantages of this system, the selectivity of the reduction may be problematic. Indeed, an incomplete reduction leads to the formation of NH$_3$ and/or N$_2$O [4], a powerful greenhouse effect gas responsible for about 6% of the anthropogenic radiative forcing [5]; besides this, N$_2$O is expected to become the most important ozone-depleting gas. It is known that the N$_2$O emission rate depends on a multitude of factors: presence, technology and age of catalyst (e.g. vehicles equipped with a three-way catalyst have higher N$_2$O emission rates than old vehicles without a catalyst); driving regime and catalyst temperature (largest emissions for cold catalyst); type of fuel; presence of sulfur in fuel; etc.; also, it is clear that N$_2$O is formed inside the catalyst as an intermediate during NO reduction [6].

In previous works of our group [7,8] we have investigated mechanistic aspects of N$_2$O formation over Pt- and Rh-based lean NO$_x$ trap catalysts by using H$_2$, NH$_3$ and CO as reductants. Micro-reactor experiments and *operando* infrared spectroscopy have been used to

---

provide a complementary overview on the pathways leading to N_2O evolution during the reduction of the stored NO_x, i.e. the so-called primary N_2O formation [9]. It has been found that the N_2O formation involves the presence of gaseous NO and originates upon the coupling of undissociated NO molecules with N-adatoms, in line with other literature works [9–12]. This process is driven by the presence of partially reduced Platinum-Group-Metal (PGM) sites, which catalyse the NO dissociation into N- and O-adspecies on one side and prevent complete NO dissociation on the other side [9,13]. Accordingly, N_2O formation is observed at low temperatures, when PGM sites are partially reduced, and is negligible at high temperatures where PGM sites are fully reduced and complete NO dissociation takes place. The onset temperature for N_2O formation depends on the activity of the reductant in the reduction of the PGM sites, i.e. upon the efficiency in the O-scavenging process by the reductant [7].

In this work we want to provide further insights into the mechanisms involved in N_2O formation over model Pt- and Rh-Ba/Al_2O_3 catalysts when a more representative reducing mixture (CO + H_2 in a 3/1 ratio) has been considered with respect to our previous studies [7,8]. Accordingly the reactivity of gaseous NO and of stored NO_x species (nitrates) has been studied using CO/H_2 reducing mixtures both under isothermal conditions and temperature programming. Complementary gas phase analysis and FT-IR characterization of the surface species are here presented, and eventually deeper insights on the N_2O formation pathways and mechanisms could be provided.

2. Experimental

The reactivity study has been performed over homemade Pt-Ba/Al_2O_3 (1/20/100 w/w) and Rh-Ba/Al_2O_3 (0.5/20/100 w/w). The catalysts have been prepared by standard incipient wetness impregnation of commercial γ-alumina support with aqueous solution of Pt$(NH_3)_2(NO_2)_2$ or Rh$(NO_3)_3$. After drying and calcination at 500 °C, the binary Pt-Al_2O_3 or Rh-Al_2O_3 samples have been impregnated with Ba$(CH_3COO)_2$ aqueous solution. After drying overnight and calcination at 500 °C for 5 h, Pt-Ba/Al_2O_3 catalyst shows a specific surface area of 131 $m^2 g^{-1}$ with a final metal dispersion near 48%; Rh-Ba/Al_2O_3 exhibits a specific surface area of 135 $m^2 g^{-1}$ with a Rh dispersion near 7%.

Lean-rich cycles have been performed using 60 mg of powder catalyst (70–100 μm) loaded in a micro-reactor (7 mm I.D.) under a flow of 100 cc/min (at 0 °C and 1 atm). During the lean phase NO/O_2 (1000 ppm NO + 3% O_2 v/v in He) has been fed to the reactor, while the rich phase consists of CO/H_2 (1500/500 ppm in He) or H_2 (2000 ppm in He). The gas exiting from the reactor were monitored by on-line mass spectrometer (QMS 200, Pfeiffer), FT-IR analyser (Multigas 2030, MKS) and μGC (Agilent).

Lean-rich experiments have also been carried out in an *operando* FT-IR reactor for the analysis of the surface species. In this case 15 mg of sample was formed into a self-supported disk with diameter 16 mm and thickness 0.11 mm. Then, square shape was cut with characteristic length 11 mm, placed inside the sample holder, and inserted into a "sandwich" IR reactor [14]. The sample holder has been fixed between KBr windows to drive the gases around the wafer with the same dynamic as in a 400 cpsi honeycomb; the temperature was measured with a K-type thermocouple, inserted 1 mm above the wafer and calibrated to provide the actual temperature in the centre of the wafer. The spectra were collected on the FT-IR Nicolet Nexus with a spectral resolution of 4 cm^{-1} and accumulation of 64 scans under atmospheric pressure using a mercury-cadmium-telluride (MCT) detector. The outlet of IR cell was measured continuously with mass spectrometer (ThermoStar TM GSD 301), chemiluminescence analyser (42i-HL MEGATEC) and FT-IR gas analyser with a MCT detector [15].

The reactivity of gaseous NO (1000 ppm in Ar) and of stored NO_x (nitrates) has also been investigated in the *operando* FT-IR cell under temperature programming (TPR and TPSR experiments) in the temperature range 40 °C–400 °C (heating rate: 4 °C/min) with various reductants, i.e. CO (2000 ppm), CO/H_2 (1500 ppm + 500 ppm), CO (2000 ppm) + H_2O (2% v/v). Before the catalytic runs the samples were subjected to the conditioning procedure in order to obtain reproducible catalyst behavior, i.e. 4–6 lean-rich cycles with NO (1000 ppm) + O_2 (3%) and H_2 (2000 ppm) in He for the lean and rich phase, respectively. Afterwards, the catalysts were subjected to cleaning treatment at 400 °C with H_2 (2000 ppm) in order to remove residual N-containing species originating from the conditioning procedure, if any.
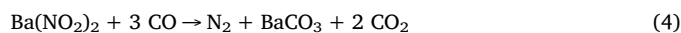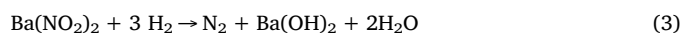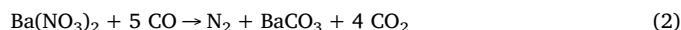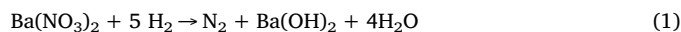
3. Results and discussion

3.1. Lean-rich cycles with CO + H_2

Fig. 1 shows the results of isothermal lean-rich cycles performed at 250 °C over Pt-Ba/Al_2O_3 and Rh-Ba/Al_2O_3 catalysts using CO + H_2 mixture or H_2 as reductant (Fig. 1A and B, respectively, for Pt-Ba/Al_2O_3 and Fig. 1C and D for Rh-Ba/Al_2O_3). Note that in the Figures only one representative lean-rich cycle has been shown, while the entire experiment consists in several lean-rich cycles.

Over Pt-Ba/Al_2O_3 when using CO + H_2 as reducing mixture (Fig. 1A), a dead time near 90 s is observed in the NO_x breakthrough upon NO/O_2 admission; then the NO_x concentration increases with time approaching a steady state value. As expected at this temperature the NO oxidation is effective and high concentration of NO_2 is detected at the reactor outlet.

The transition to the rich phase leads to the reduction of the stored NO_x species. Indeed, upon feeding the CO + H_2 reducing mixture, N_2 is immediately formed together with CO_2. Initially the reductant is completely consumed and the N_2 concentration remains constant; then, the N_2 concentration decreases and CO and H_2 breakthrough is observed along with NH_3. Formation of N_2 could be described by the following global reactions in the case of nitrates and nitrites, respectively:

$$Ba(NO_3)_2 + 5\ H_2 \rightarrow N_2 + Ba(OH)_2 + 4H_2O \tag{1}$$

$$Ba(NO_3)_2 + 5\ CO \rightarrow N_2 + BaCO_3 + 4\ CO_2 \tag{2}$$

$$Ba(NO_2)_2 + 3\ H_2 \rightarrow N_2 + Ba(OH)_2 + 2H_2O \tag{3}$$

$$Ba(NO_2)_2 + 3\ CO \rightarrow N_2 + BaCO_3 + 2\ CO_2 \tag{4}$$

NH_3 evolution is then observed after N_2 formation, in line with the suggested 2-steps reduction mechanism involving the formation of ammonia as intermediate species in N_2 formation [16,17].

Notably, N_2O formation is also observed in correspondence to both the lean-to-rich and rich-to-lean transitions (primary and secondary N_2O formation, respectively), as also reported by other studies [9,10]. In particular during this experiment a rather small N_2O peak is observed at the lean-to-rich transition (primary N_2O formation), whereas a much greater N_2O peak is seen upon the rich-to-lean switch.

N_2O formation upon the lean to rich transition (primary N_2O) is related to the reaction of NO, released in the gas phase from the NO_x adsorbed species, over partially reduced metal sites (Me = Pt, Rh) [7,9]:

$$NO + 2\ Me \rightarrow Me\text{-}N + Me\text{-}O \tag{5}$$

$$NO + Me\text{-}N \rightarrow N_2O + Me \tag{6}$$
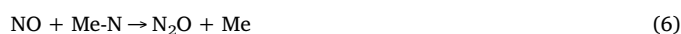
and the resulting O adspecies are scavenged by the reductant:

$$Me\text{-}O + Me\text{-}CO \rightarrow 2\ Me + CO_2 \tag{7}$$

$$Me\text{-}O + 2\ Me\text{-}H \rightarrow 3\ Me + H_2O \tag{8}$$

At variance, formation of secondary N_2O (rich to lean transition) is related to the reaction of adsorbed NCO^- (isocyanate species) with NO/O_2 [18] and/or to the reaction of adsorbed CO with NO. This clearly
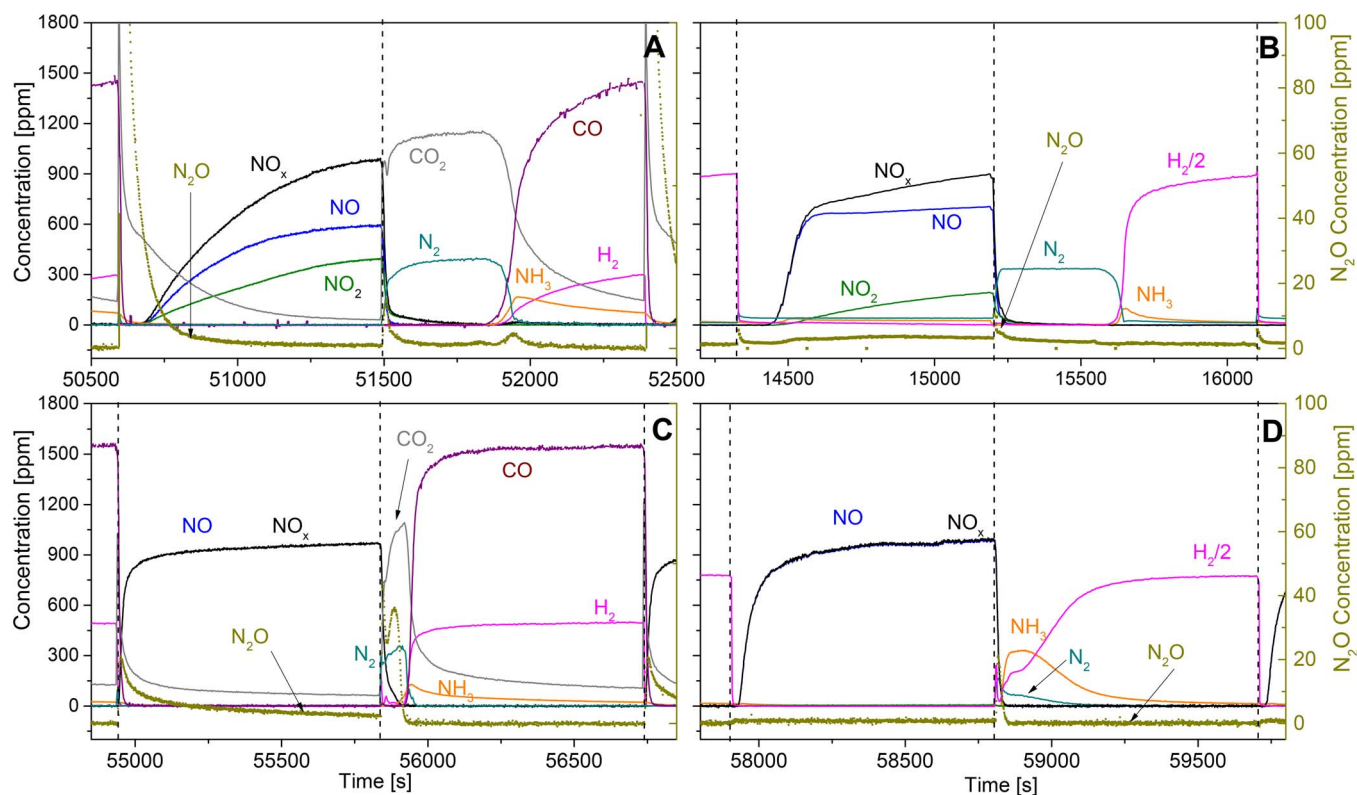
Fig. 1. Lean-rich cycles at 250 °C over Pt-Ba/Al$_2$O$_3$ (A: rich phase in CO + H$_2$; B: rich phase in H$_2$) and Rh-Ba/Al$_2$O$_3$ (C: rich phase in CO + H$_2$; D: rich phase in H$_2$). Lean conditions: NO 1000 ppm + O$_2$ 3% v/v in He, length 15 min; rich conditions: CO 1500 ppm + H$_2$ 500 ppm in He, or H$_2$ 2000 ppm in He, length 15 min.

appears from FT-IR spectra recorded during the rich and lean phases (Fig. 2A and B, respectively. Only the 1800–2500 cm^{-1} region is shown). During the rich phase (Fig. 2A) the bands characteristic of CO adsorbed on Pt (2043 cm^{-1}) and of isocyanates NCO$^-$ species on Al^{3+} tetrahedrally and octahedrally coordinated, respectively (2230, 2245 cm^{-1}) [19] and Ba phase (2170 cm^{-1}) [20] rapidly grow up; these species are formed upon the reduction of stored NO$_x$ with CO [21]. Then, upon switching to the lean phase (Fig. 2B), the band of adsorbed CO on Pt immediately disappears whereas those of isocyanates decrease more slowly. Simultaneously, N$_2$O evolution is observed, suggesting that its formation is related to the reaction of NCO$^-$ with NO/O$_2$ [22] and/or to the reaction of adsorbed CO with NO. Note that the oxidation of isocyanates is not complete since residual NCO$^-$ species remain on the catalyst surface at the end of the lean phase.

Lean-rich cycles have been performed at the same temperature using H$_2$ as reductant as well, and results are shown in Fig. 1B. A slightly higher dead time for NO$_x$ breakthrough is observed if compared to Fig. 1A. Switching from lean to rich conditions a similar products evolution is observed, with instantaneous production of N$_2$ and of NH$_3$ later on. Primary and secondary N$_2$O peaks are detected also in this case upon the lean-to-rich and rich-to-lean switches respectively, although they are almost negligible at variance with that observed in the case of CO/H$_2$ as reducing mixture. In particular, negligible amounts of secondary N$_2$O are detected when using H$_2$ as reducing agent. According to the lines previously depicted, this is due to the lack of isocyanate species whose formation is not possible in this case and that in fact have not been observed by FT-IR spectroscopy (data not reported).

Lean-rich cycles at 250 °C using CO + H$_2$ mixture or H$_2$ as reductant have been carried out also over the Rh-Ba/Al$_2$O$_3$ catalyst and representative cycles are reported in Fig. 1C and D, respectively. The Rh-based catalyst exhibits a lower storage capacity than the Pt-based catalyst, as pointed out by the lower dead time for NO$_x$ breakthrough. Also, the NO oxidation capability is very poor. The lower storage capacity of the Rh-containing catalyst, together with its lower NO

oxidizing capabilities, might be related to the lower noble metal dispersion of this system compared to the Pt-based catalyst sample, as reported in the Experimental section. This is in line with the observation that i) the storage ability of Pt-containing catalysts increases upon increasing the metal dispersion [23], and ii) an higher storage capacity is in fact obtained at these temperatures when the Rh dispersion is higher than that of Pt [7].

The reduction phases over Rh-Ba/Al$_2$O$_3$ catalyst show similar features to those described in the case of Pt-Ba/Al$_2$O$_3$ catalyst. Upon admission of CO + H$_2$ or H$_2$, the stored NO$_x$ are reduced to N$_2$, N$_2$O and NH$_3$. Also in this case, a significant production of N$_2$O is observed at the lean-to-rich transition (primary N$_2$O) in the presence of CO + H$_2$, and a minor formation in the presence of H$_2$ only.

N$_2$O formation is observed at the rich-to-lean transition as well (secondary N$_2$O) in the case of the CO/H$_2$ reducing mixture (Fig. 1C), although in much lower amounts if compared to Pt-Ba/Al$_2$O$_3$. Again, this is due to the reaction of NO/O$_2$ with isocyanate species/adsorbed CO, as pointed out by the spectra reported in Fig. 2C showing the formation of isocyanates on Ba and Al sites (bands at 2170, 2230, 2245 cm^{-1}) during the rich phase, along with adsorbed CO on Rh sites (CO dicarbonyls on Rh$^+$ at 2084 and 2010 cm^{-1} [20] and Rh$^+$ monocarbonyl or Rh$^+$(CO)(NO) complex at 2048 cm^{-1} [24]), being the intensity of these latter lower than in the case of Pt. When switching to the lean phase (Fig. 2D) the bands of isocyanates decrease due to the oxidation of these species by NO/O$_2$, and a N$_2$O peak is detected in the gas phase (Fig. 1C).

The effect of temperature on N$_2$O formation is shown in Fig. 3A (Pt-based catalyst) and 3B (Rh-based catalyst), where the amounts of N$_2$O evolved during the lean-to-rich and rich-to-lean transitions are shown at 250 °C and 350 °C when both CO/H$_2$ mixtures and pure H$_2$ are used as reducing agents. In all cases both the primary and the secondary N$_2$O peaks decrease by increasing the temperature. Furthermore, higher amounts of N$_2$O are formed when CO/H$_2$ is used as reducing mixture, and in particular during the secondary N$_2$O formation. Accordingly, the
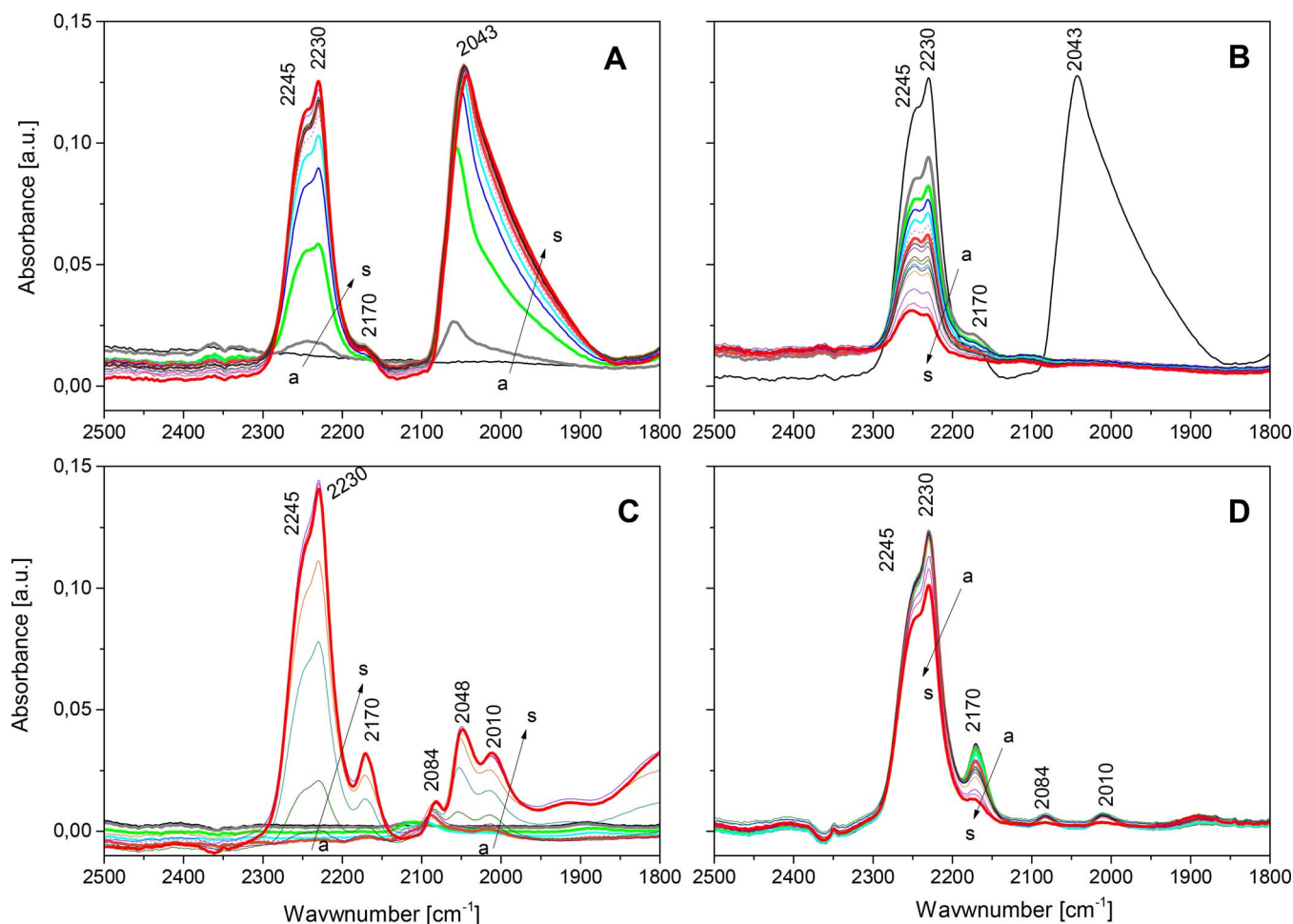
Fig. 2. *Operando* FTIR spectra during lean-rich cycles at 250 °C over Pt-Ba/Al$_2$O$_3$ (A: first rich phase in CO + H$_2$; B: subsequent lean phase in NO/O$_2$) and Rh-Ba/Al$_2$O$_3$ (C: first rich phase in CO + H$_2$; D: subsequent lean phase in NO/O$_2$). Spectra collected every 0.2 s up to 10 min.

nitrogen selectivity increases upon increasing the temperature since in all cases both the amounts of NH$_3$ and of N$_2$O decrease.

The data presented so far showed that over both the Pt- and Rh-based catalytic systems N$_2$O formation is observed both during lean-to-rich (primary) and rich-to-lean (secondary) transitions, in line with literature reports [9,11 and references therein]. Higher amounts of N$_2$O (both primary and secondary N$_2$O) are formed when CO/H$_2$ is used as

reducing mixture if compared to pure H$_2$. Besides, temperature also affects N$_2$O formation, being N$_2$O emissions higher at lower temperatures. To better clarify mechanistic aspects involved in N$_2$O formation in the presence of CO, and on the role of the noble metal on its formation, the reduction of stored nitrates and gas-phase NO with CO and CO/H$_2$ mixtures has been investigated under temperature programmed conditions.
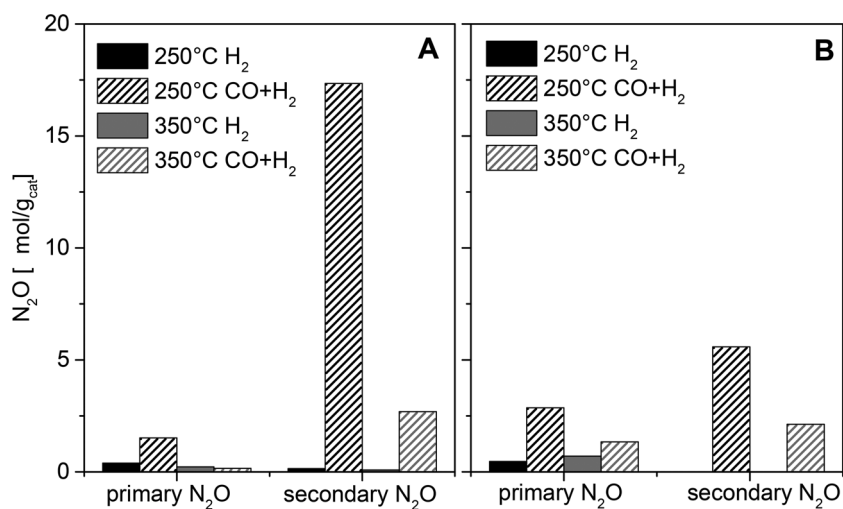

Fig. 3. Total amount of N$_2$O produced during lean-rich cycles at 250 °C over A) Pt-Ba/Al$_2$O$_3$ catalyst; B) Rh-Ba/Al$_2$O$_3$ catalyst.
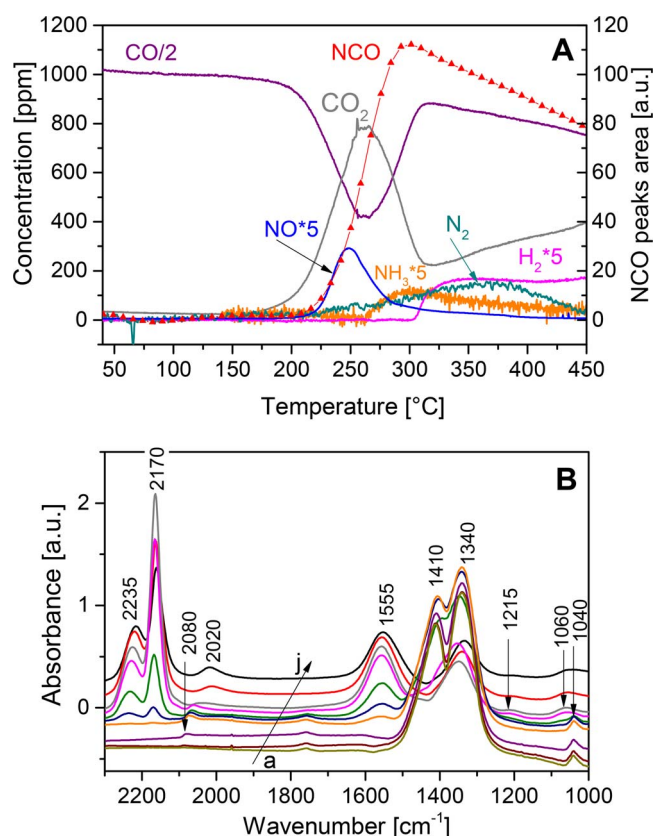
Fig. 4. A) TPSR experiments with CO (2000 ppm) over Pt-Ba/Al$_2$O$_3$ after NO (1000 ppm)/O$_2$ (3%) adsorption at 350 °C; B) *operando* FTIR spectra during TPSR experiments. Spectra collected at: a) 40 °C; b) 74 °C; c) 124 °C; d) 199 °C; e) 225 °C; f) 250 °C; g) 275 °C; h) 301 °C; i) 378 °C; j) 450 °C. NCO chemigram has been calculated from NCO peaks area (band at 2235 cm^{-1} and 2170 cm^{-1} in panel B).

Fig. 5. A) TPSR experiments with CO (2000 ppm) over Rh-Ba/Al$_2$O$_3$ after NO (1000 ppm)/O$_2$ (3%) adsorption at 350 °C; B) *operando* FTIR spectra during TPSR experiments. Spectra collected at: a) 40 °C; b) 121 °C; c) 211 °C; d) 244 °C; e) 260 °C; f) 268 °C; g) 294 °C; h) 376 °C; i) 450 °C. NCO chemigram has been calculated from NCO peaks area (band at 2230 cm^{-1} and 2167 cm^{-1} in panel B).

3.2. CO-TPSR of nitrates

The reactivity of nitrate ad-species stored over Pt- and Rh-based catalysts has been investigated under temperature programming using CO as reductant (CO-TPSR). The results of the gas phase analysis are reported in Figs. 4A and 5A for Pt- and Rh-based catalysts, respectively, whereas Figs. 4B and 5B show the corresponding surface species on the catalyst obtained with *operando* FT-IR spectroscopy. Figs. 4A and 5A report also the surface concentration of isocyanate species, obtained by integration of the area of the peaks in the FT-IR spectra with maxima at 2230–2235 cm^{-1} and 2167–2170 cm^{-1}.

Over Pt-Ba/Al$_2$O$_3$ catalyst (Fig. 4A), the temperature onset for CO consumption is observed near 175 °C with simultaneous CO$_2$ evolution. CO consumption is also accompanied by evolution of NO and N$_2$, observed starting from 220 °C, and by isocyanates formation, as shown by FT-IR spectra of Fig. 4B (see below). The isocyanate concentration trace as a function of temperature is also shown in Fig. 4A. Above 250–300 °C small amounts of ammonia are also detected, along with trace amounts of H$_2$, possibly related to the reaction of CO with surface hydroxyls (WGS reaction).

Very similar results have been obtained in the case of Rh-Ba/Al$_2$O$_3$ catalyst (Fig. 5A) although the CO consumption (and the evolution of reaction products) is minor if compared to the Pt-based sample due to the lower amounts of initially stored NO$_x$. Also, NCO$^-$ species are formed to a lower extent. Notably, in both case no N$_2$O has been found at the reactor outlet.

The FT-IR analysis of the surface species performed over Pt-Ba/Al$_2$O$_3$ catalyst during the CO-TPSR is shown in Fig. 4B. Curves a–j correspond to the spectra recorded upon heating the stored nitrates with CO in the 40–450 °C temperature range. Upon heating, the bands
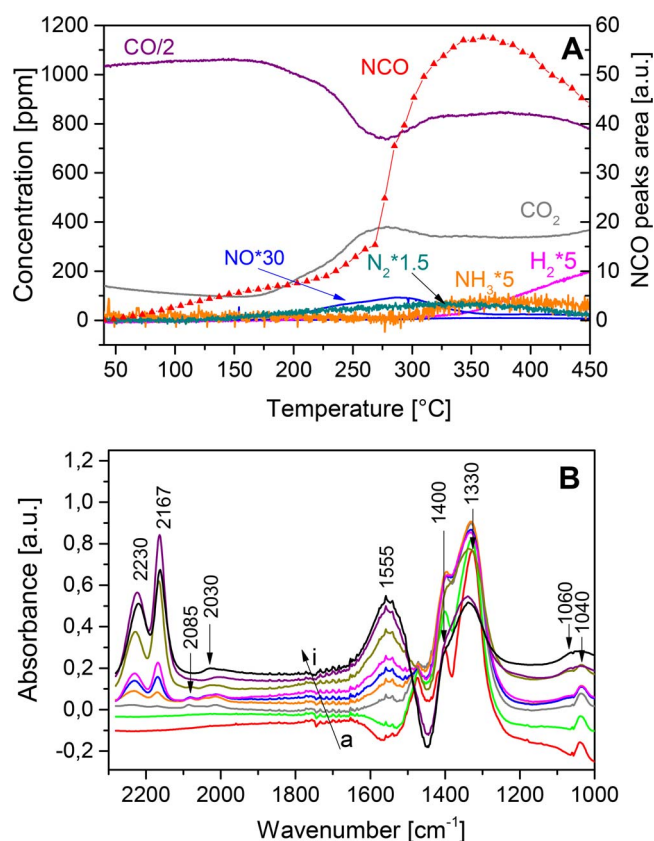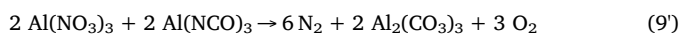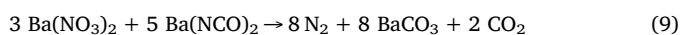
of surface nitrates (modes at 1340 cm^{-1}, 1410 cm^{-1} and 1040 cm^{-1}) remain unchanged up to ca. 200 °C and then rapidly decrease. Starting from 200 °C, NCO$^-$ species are formed on Al and Ba sites [21], as revealed by the two related bands at 2235 and 2170 cm^{-1}, whose intensity increases markedly with temperature, while the position slightly shifts to lower frequencies. The formation of NCO$^-$ species is accompanied by the formation of carbonates: main bands are observed at 1555, ~ 1340 and 1065 cm^{-1} even if the partial superposition of vibrational modes of carbonates and nitrates makes it difficult to track the simultaneous NO$_x$ removal and carbonates formation. However, the analysis of the spectra at lower wavenumbers clearly show that the ν1 mode band at 1040 cm^{-1} (related to nitrates) decreases while a shoulder at 1060 cm^{-1} progressively appears due to carbonate formation.

The formation of small amounts of nitrites (low intensity band at 1215 cm^{-1}) is also observed upon reduction of nitrates. Furthermore, FT-IR spectra also show the presence of a weak band at ca. 2080 cm^{-1} (shifting towards 2020 cm^{-1} with temperature) related to the presence of linear carbonyls onto the Pt sites and witnessing for a progressive reduction of the metal particles or the reduction of the metal particle sizes (surface restructuring) [25]. NCO$^-$ species (bands at 2170 and 2235 cm^{-1}) are thermally stable and are still present on the catalyst surface at the end of the heating ramp (see the concentration trace of NCO$^-$ species showed in Fig. 4A).

The FT-IR spectra recorded over Rh-Ba/Al$_2$O$_3$ catalyst during the CO-TPSR of nitrates (Fig. 5B) show similar features with respect to those already described for Pt-catalyst. At the beginning nitrates species are present at catalyst surface (main bands in the range 1400–1330 cm^{-1} and at 1040 cm^{-1}). Upon increasing the temperature, nitrates bands decrease and Ba-carbonates (main band at 1555 cm^{-1})

are formed, along with Rh-dicarbonyls (bands at ca. 2085 and 2010 cm^{-1}, shifting towards 2030 cm^{-1} with temperature). Also in this case the analysis of IR modes in the 1500–1300 cm^{-1} is not straightforward because of the superposition of vibrational modes of carbonates and nitrates. The consumption of nitrates is accompanied by the increase of bands at 2167 and 2230 cm^{-1}, related to isocyanates formation. Also in this case the formation of NCO^{-} species increases with temperature and at the end of the heating ramp significant amounts of isocyanate species are present onto the surface (see also the NCO^{-} concentration trace in Fig. 5A).

The results reported above clearly indicate that the reduction of stored nitrates with CO leads to the formation of both gaseous (NO, N_2, NH_3) and adsorbed species (isocyanates), in line with previous works carried out over the same Pt-Ba/Al_2O_3 sample [21]. In particular, from Figs. 4 and 5 it appears that isocyanate species are initially formed upon reaction of CO with the surface nitrates and the consequent release of NO; then N_2 formation is observed upon surface reaction involving isocyanates and nitrates and/or NO according to the stoichiometry of the overall reactions (9), (9') and (10), (10'):

$$3\ Ba(NO_3)_2 + 5\ Ba(NCO)_2 \rightarrow 8\ N_2 + 8\ BaCO_3 + 2\ CO_2 \qquad (9)$$

$$2\ Al(NO_3)_3 + 2\ Al(NCO)_3 \rightarrow 6\ N_2 + 2\ Al_2(CO_3)_3 + 3\ O_2 \qquad (9')$$

$$6\ NO + 2\ Ba(NCO)_2 \rightarrow 5\ N_2 + 2\ BaCO_3 + 2\ CO_2 \qquad (10)$$

$$6\ NO + 2\ Al(NCO)_3 \rightarrow 6\ N_2 + Al_2(CO_3)_3 + 3\ CO \qquad (10')$$

Worth to note is the absence of N_2O in the reduction products during these experiments, indicating that the reduction of the stored nitrates with CO is selective to NO and N_2 (and isocyanates). This is possibly related to the small concentration of gas-phase NO that is released in the gas phase from the adsorbed NO_x species, as discussed below.

3.3. NO/CO-TPR

To better clarify the role of gas phase NO and NCO^{-} ad-species in the N_2O formation, experiments have been performed by feeding CO/NO mixtures over Pt-Ba/Al_2O_3 and Rh-Ba/Al_2O_3 (TPR experiments). The results of the gas phase analysis are shown in Figs. 6A and 7A for the Pt-Ba/Al_2O_3 and Rh-Ba/Al_2O_3 catalysts, respectively, while the surface analyses are shown in Figs. 6B and 7B.

Over Pt-Ba/Al_2O_3, the onset temperature for NO and CO consumption is detected near 150 °C, accompanied by the formation of small amounts of N_2 and N_2O (Fig. 6A) and of isocyanates (Fig. 7A and trace in Fig. 6A). The CO concentration profile decreases with temperature and shows a minimum near 300 °C, whereas that of NO shows a monotonic decrease. NO is completely consumed above 350 °C. Among the reduction products, N_2O shows a maximum near 330 °C whereas N_2 presents a monotonic increase. Small amount of NH_3 are also formed. The parallel surface characterization (Fig. 6B) shows the development of several bands upon increasing the temperature, and in particular: i) bands at 2167 cm^{-1} and 2227 cm^{-1} attributed to NCO^{-} species on barium and alumina sites, respectively [26]; ii) bands near 1610 cm^{-1} (shift towards 1555 cm^{-1}) and 1330 cm^{-1} corresponding to bidentate carbonates on alumina (doubly degenerated ν_{asym} (OCO) stretch), iii) 1443 cm^{-1} and 1394 cm^{-1} attributed to monodentate and/or bulk ionic carbonates [26,27]; iv) band at 1214 cm^{-1} (low intensity) corresponding to nitrites. Above 170 °C new peaks of carbonates are also observed at 1060 cm^{-1} [ν_{sym} (OCO) mode] together with 1360 cm^{-1} (monodentate and/or bulk ad-species). Furthermore, FT-IR spectra also show the presence of a weak band near 2085 cm^{-1} (shift towards 2060 cm^{-1}) corresponding to carbonyls bonded to Pt. Of note, at the end of the temperature ramp, significant amounts of isocyanates species remain on the surface (see Fig. 6A and B). As a matter of facts, the instantaneous C- and N-balance (not shown in the Figure) shows negative deviation in the range 250–400 °C due to the build-up of
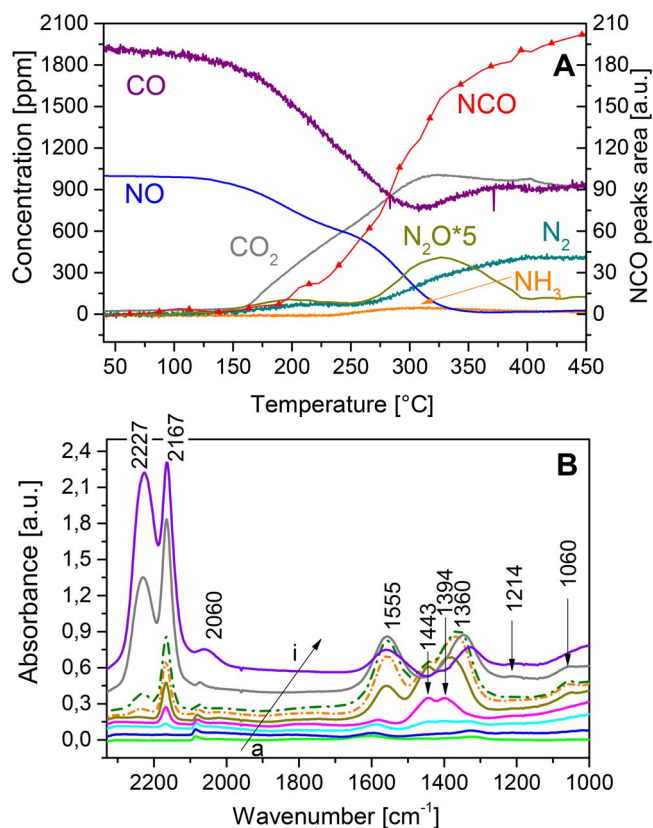

Fig. 6. A) TPR experiment over Pt-Ba/Al_2O_3 catalyst from 40 to 400 °C (4 °C/min), with NO (1000 ppm) + CO (2000 ppm); B) *operando* FTIR spectra during TPR. Spectra collected at a) 40 °C, b) 79 °C; c) 121 °C; d) 146 °C; e) 172 °C; f) 192 °C; g) 223 °C; h) 300 °C; i) 400 °C. NCO chemigram has been calculated from NCO peaks area (band at 2227 cm^{-1} and 2167 cm^{-1} in panel B).

isocyanate species on the surface.

A similar picture is obtained over the Rh-Ba/Al_2O_3 catalyst, but the NO + CO reaction is observed at higher temperatures. However the NO consumption is completed at lower temperatures in this case. In fact the gas phase analysis (Fig. 7A) shows a NO light off temperature near 220 °C, with production of N_2 and N_2O. Isocyanates species are also formed, but at much lower concentration if compared to Pt-Ba/Al_2O_3. N_2O presents a maximum in the concentration near 275 °C, while complete NO consumption is observed near 300 °C. Also in this case, small amounts of ammonia are detected. The corresponding surface spectra obtained over Rh-catalyst (Fig. 7B) show a small band near 1218 cm^{-1} due to nitrites formation at the very beginning of the heating rate which then decreases with temperature. Above 250 °C, the development of bands at 2165 and 2227 cm^{-1} indicates the formation of NCO^{-} species. By increasing the temperature, these bands grow together with those of Rh-CO (2077 and 2005 cm^{-1}) and superficial Ba-carbonates (main bands at ca. 1555, 1350 and 1060 cm^{-1}). At the end of the run, the surface of the catalyst is dominated by CO- and NCO-ad-species, although the intensity of NCO^{-} modes is much lower with respect to Pt-based catalyst. As a matter of facts, in this case the instantaneous C- and N-balance show only a small negative deviation in the range 250–350 °C (not shown in the Figure), due to the minor build-up of isocyanate species. The NCO^{-} species are still present onto the catalyst surface at the end of the heating ramp.

The following overall reactions may be invoked to account for the formation of the reaction products over both Pt- and Rh-catalysts in the CO + NO reaction:
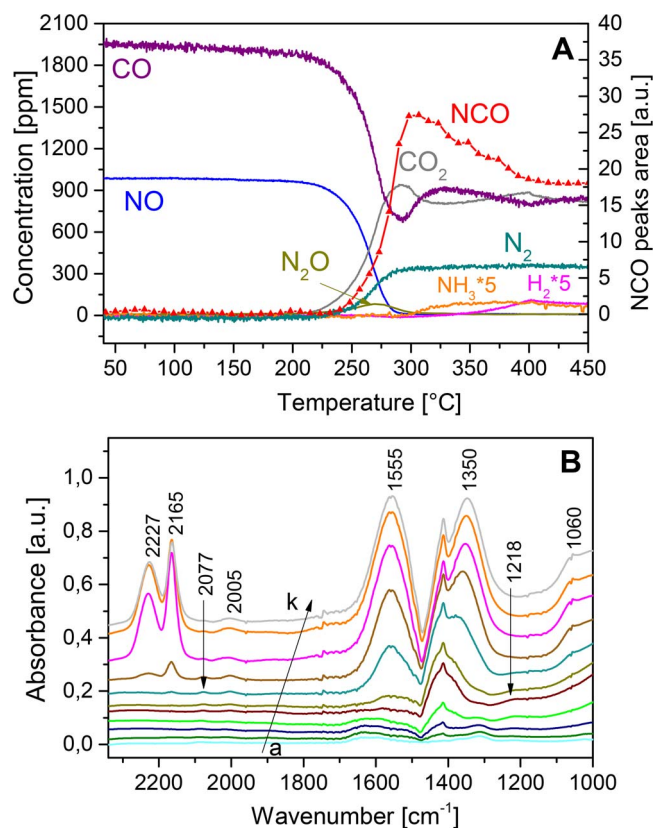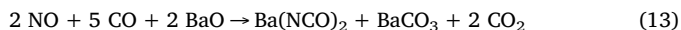
$$2\ NO + CO \rightarrow N_2O + CO_2 \qquad (11)$$

Fig. 7. A) TPR experiment over Rh-Ba/Al$_2$O$_3$ catalyst from 40 to 400 °C (4 °C/min), with NO (1000 ppm) + CO (2000 ppm); B) *operando* FTIR spectra during TPR. Spectra collected at a) 40 °C; b) 77 °C; c) 101 °C; d) 142 °C; e) 167 °C; f) 209 °C; g) 251 °C; h) 301 °C; i) 326 °C; j) 351 °C; k) 400 °C. NCO chemigram has been calculated from NCO peaks area (band at 2227 cm^{-1} and 2165 cm^{-1} in panel B).

$$2\ NO + 2\ CO \rightarrow N_2 + 2\ CO_2 \tag{12}$$

$$2\ NO + 5\ CO + 2\ BaO \rightarrow Ba(NCO)_2 + BaCO_3 + 2\ CO_2 \tag{13}$$

$$6\ NO + 6\ CO + 2\ Al_2O_3 \rightarrow 2\ Al_2(NCO)_3 + 6\ O_2 \tag{13'}$$
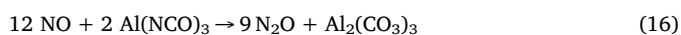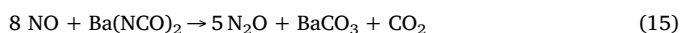
Note that both the Pt- and Rh-catalyst show similar features, with different onset temperatures being Rh- generally less active than the Pt-based sample.

Notably, over the Pt-Ba/Al$_2$O$_3$ catalyst sample, the production of N$_2$O is observed both in the low-temperature region with a maximum near 200 °C, and at high-temperature with a maximum near 300 °C. It should be speculated that at low temperature, gaseous NO fed to the reactor reacts with reduced Pt sites giving N$_2$O according to the reactions (5)–(7) already discussed. Since undissociated NO molecules are involved in these reactions, the catalyst metal sites should be not fully reduced in order to prevent complete NO dissociation.

Oxygen formed by the direct dissociation of NO on reduced Pt atoms or concomitant to isocyanate formation (reaction (13')) can produce N$_2$O as well, according to reaction (14) [19]:

$$2\ NCO + 3/2\ O_2 \rightarrow N_2O + 2\ CO_2 \tag{14}$$

On the other hand, at high-temperatures the reaction between isocyanate species and gaseous NO may also contribute to N$_2$O formation:

$$8\ NO + Ba(NCO)_2 \rightarrow 5\ N_2O + BaCO_3 + CO_2 \tag{15}$$

$$12\ NO + 2\ Al(NCO)_3 \rightarrow 9\ N_2O + Al_2(CO_3)_3 \tag{16}$$

In the case of Rh-based sample, the formation of N$_2$O occurs only at low temperatures through the reaction between gaseous NO and the reduced metal sites (reactions (5)–(6)) and not at high temperature due to the low amounts of isocyanate species present at the surface (see
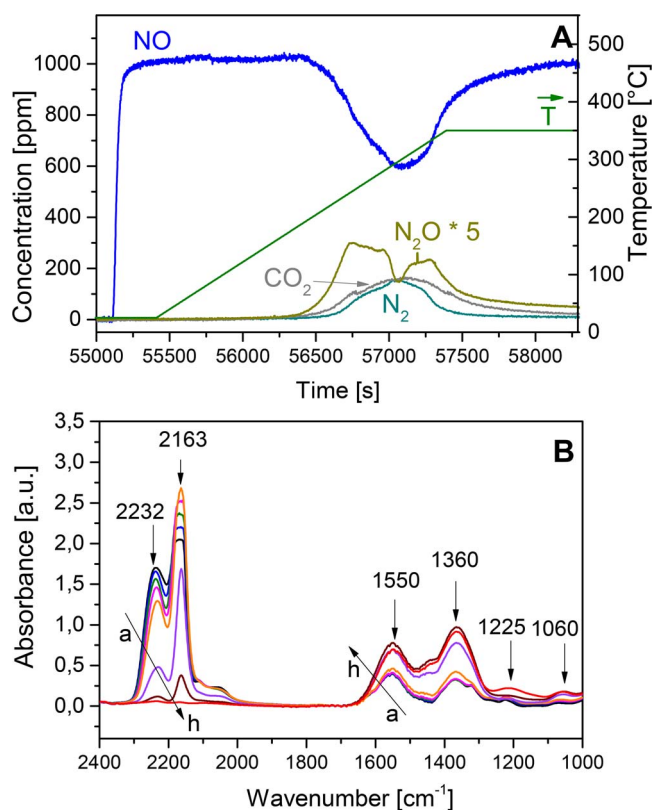
Fig. 8. A) TPSR experiment with NO (1000 ppm) over Pt-Ba/Al$_2$O$_3$ from r.t. to 350 °C (10 °C/min), after NO/CO TPR; B) *operando* FTIR spectra during TPSR experiment. Spectra collected at a) 50 °C; b) 100 °C; c) 150 °C; d) 200 °C; e) 250 °C; f) 300 °C; g) 325 °C; h) 350 °C.

Fig. 7A). We can consider too that the few residual isocyanates are hydrolyzed into ammonia, which appears from 300 °C.

The comparison between the results obtained during TPSR and TPR experiments, where NO$_x$ stored species or gaseous NO respectively react with fed CO, clearly confirm that the formation of N$_2$O is favored by the presence of high gas-phase concentration of NO. In fact NO is involved in N$_2$O formation both via reactions (5)–(6) (self-coupling of NO [7,8,28]) and/or upon reaction with isocyanates (reactions (15) and (16) [29]). Both pathways require gas-phase NO; in the case of TPSR experiments (where gaseous NO is not fed to the reactor) only tiny amounts of NO are released in the gas-phase during the reduction of the stored nitrates and accordingly no N$_2$O formation is observed during the run.

In order to provide further insights into the NO/isocyanate reaction, *operando* FT-IR experiments have been carried out over Pt-Ba/Al$_2$O$_3$ where isocyanate species have been formed onto the catalyst surface by feeding NO/CO. Then, the catalyst has been cooled down to room temperature in inert atmosphere (i.e. He) and NO has been admitted to the reactor. Eventually the catalysts have been heated from RT up to 350 °C in the presence of NO, and the obtained results are shown in Fig. 8A (gas phase) and 8 B (surface). NO consumption is seen starting from ca. 200 °C (Fig. 8A) with simultaneous N$_2$O formation which is also accompanied by the evolution of N$_2$. Simultaneously CO$_2$ is detected at the reactor outlet. The correspondent FT-IR results are shown in Fig. 8B where curves a–h correspond to the spectra recorded during interaction of the NCO-ad-species previously formed (bands at 2232 cm^{-1} – isocyanates on Al^{3+} sites and 2163 cm^{-1} – isocyanates on Ba^{2+} sites, [26]) with NO in the range 50–350 °C. Upon increasing the temperature, the band at 2232 cm^{-1} is gradually eroded, while the band at 2163 cm^{-1} initially increases. This indicates the consumption of isocyanates but also the possible initial conversion of the NCO$^-$ species related to the higher frequency component into the lower
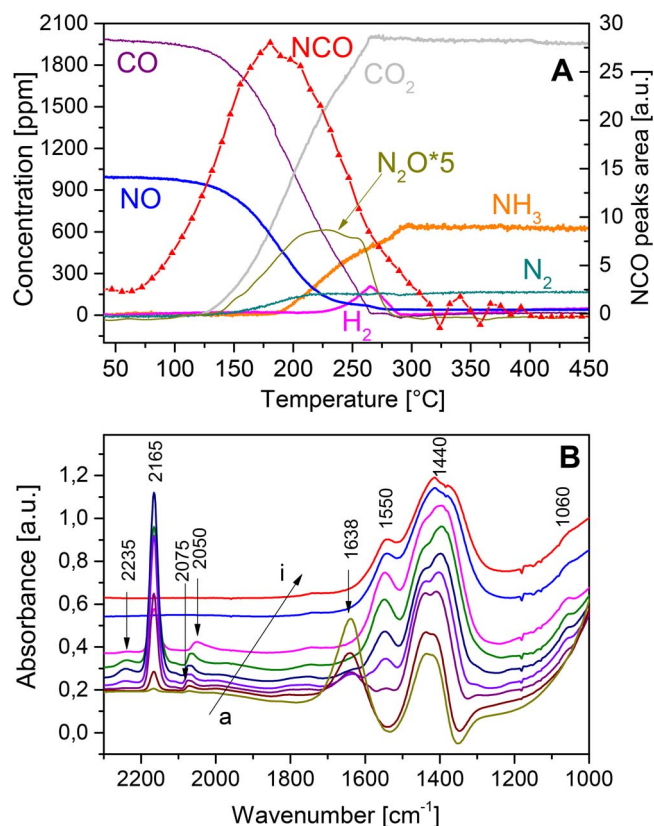
Fig. 9. A) TPR experiment over Pt-Ba/Al$_2$O$_3$ catalyst from 40 to 400 °C (4 °C/min), with NO (1000 ppm) + CO (2000 ppm) + H$_2$O (2% v/v); B) *operando* FTIR spectra during TPR. Spectra collected at a) 40 °C; b) 72 °C; c) 123 °C; d) 147 °C; e) 180 °C; f) 223 °C; g) 272 °C; h) 375 °C; i) 400 °C. NCO chemigram has been calculated from NCO peaks area (band at 2235 cm^{-1} and 2165 cm^{-1} in panel B).

Fig. 10. A) TPR experiment over Rh-Ba/Al$_2$O$_3$ catalyst from 40 to 400 °C (4 °C/min), with NO (1000 ppm) + CO (2000 ppm) + H$_2$O (2% v/v); B) *operando* FTIR spectra during TPR. Spectra collected at a) 40 °C; b) 75 °C; c) 175 °C; d) 225 °C; e) 258 °C; f) 300 °C; g) 351 °C; h) 400 °C. NCO chemigram has been calculated from NCO peaks area (band at 2230 and 2165 cm^{-1} in panel B).

frequency one. Above 250 °C the intensity of both bands decreases markedly with temperature and then are fully consumed at the end of the heating ramp. Simultaneously, the intensity of the band at 2055 cm^{-1} related to the presence of carbonyls onto Pt sites (formed during the previous NO/CO TPR) decrease with temperature, while the bands related to surface carbonates (1555, 1360 and 1060 cm^{-1}) increase due to the adsorption of CO$_2$ produced during the reaction. A small band at about 1225 cm^{-1} is also observed, indicating the formation of small amounts of nitrites. Therefore, these experiments provided evidence for the reaction of gaseous NO with surface isocyanates (and possibly adsorbed CO) to give N$_2$O.

3.4. Effect of water in the CO/NO reaction

The effect of water on the CO/NO reaction has been investigated through TPR experiments in the presence of 2% H$_2$O in the feed. Results have been reported in Figs. 9A and 10A (gas phase analysis) and Figs. 9B and 10B (surface analysis) in the case of Pt- and Rh-based catalysts, respectively.

The onset temperature for CO consumption is observed slightly above 120 °C in the case of Pt- and near 170 °C in the case of Rh-catalyst (Figs. 9A and 10A, respectively). Simultaneously, N$_2$O and N$_2$ are produced while NH$_3$ appears at slightly higher temperature (180 °C for Pt-, 225 °C for Rh-catalyst). Complete consumption of NO is reached near 270 °C both over Pt-Ba/Al$_2$O and Rh-Ba/Al$_2$O$_3$.

Over both the systems H$_2$ evolution is also observed, starting from 265 to 270 °C. The production of H$_2$ is related to the occurrence of WGS reaction due to the co-presence of CO and water:
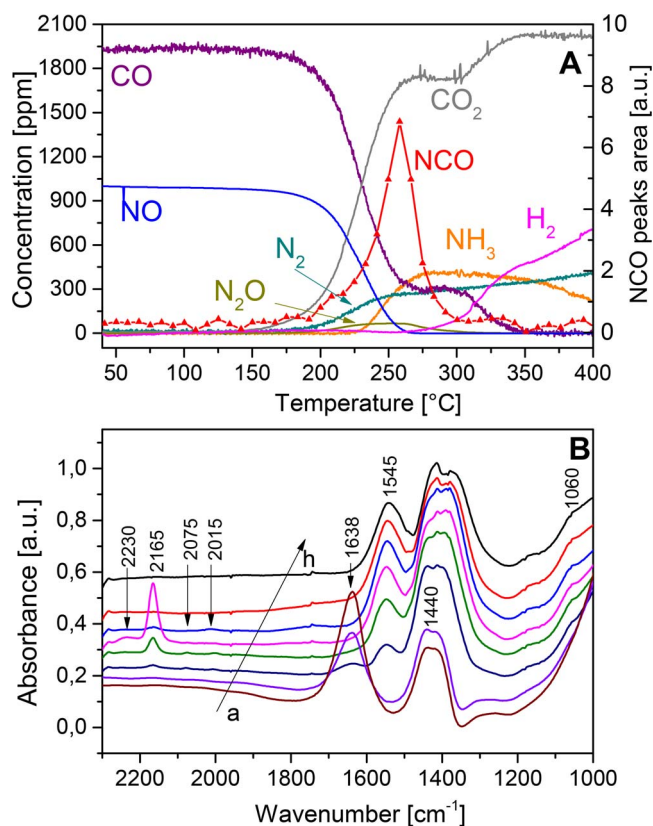
$$CO + H_2O \rightarrow H_2 + CO_2 \qquad (17)$$

In the case of the Pt-based catalyst (Fig. 9A), the H$_2$ concentration shows a maximum near 200 ppm at 270 °C. In fact H$_2$ is initially produced according to the WGS reaction (17), but it is then fully consumed in the reduction of NO. At variance in the case of the Rh-based catalyst (Fig. 10A) the H$_2$ concentration shows a monotonic increase due to the occurrence at high temperature of the NH$_3$ decomposition (reaction (18)) leading to N$_2$ and H$_2$ evolution:

$$2\, NH_3 \rightarrow N_2 + 3\, H_2 \qquad (18)$$
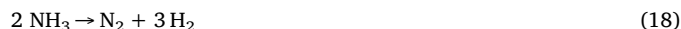
The surface analysis reported in Figs. 9B and 10B shows similar features over both catalysts: i) at low temperatures, the H$_2$O bending mode is detected at 1638 cm^{-1}; ii) bands in the region of 1700–1000 cm^{-1} reveal the formation of mainly Ba-carbonates; Pt-carbonyls bands develop in the region near 2090–2005 cm^{-1}; iv) bands corresponding to NCO$^-$ group on Ba phase appear (main band at 2165 cm^{-1}). Upon heating, Ba-carbonates evolve changing their structure and the corresponding wavenumber region shows different bands, as already discussed. On the other hand, the bands of NCO$^-$ species grow up with temperature, reach a maximum (near 180 °C and 260 °C in the case of Pt- and Rh-catalyst, respectively), and then decrease; these species appear fully consumed above 300 °C.

Comparing these data with the results obtained in the absence of water, noticeable differences are apparent. At first, the onset temperature of NO + CO reaction is shifted towards lower temperature in the presence of water, possibly due to H$_2$ formation via the reverse water gas shift reaction (in fact the reaction NO + H$_2$ reaction has a lower onset temperature). However at these temperatures the amounts of H$_2$ produced are entirely consumed in the reaction with NO leading to N$_2$O, whose formation in fact is observed at low temperatures. Also, isocyanates concentration shows a maximum with temperature being
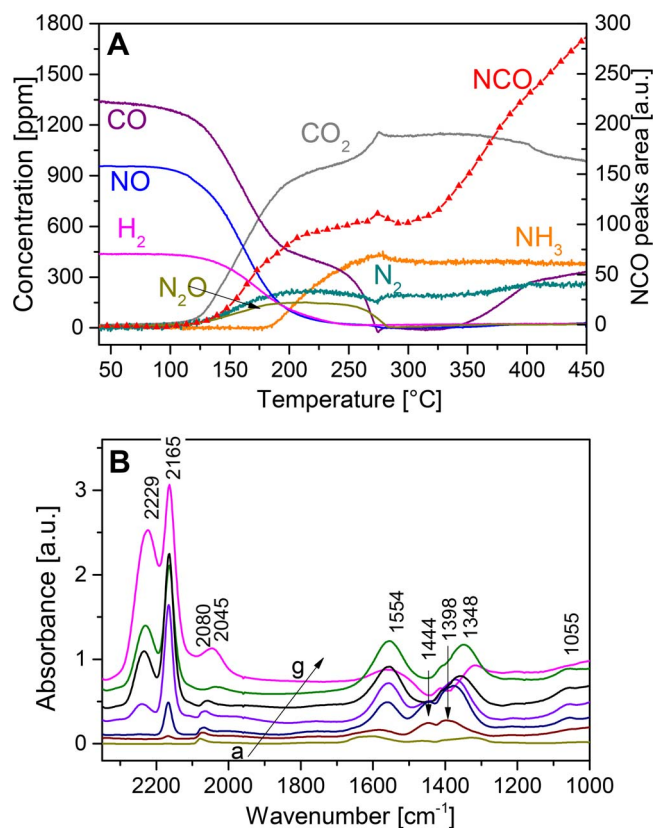
Fig. 11. A) TPR experiment over Pt-Ba/Al$_2$O$_3$ catalyst from 40 to 400 °C (4 °C/min), with NO (1000 ppm) + CO (1500 ppm) + H$_2$ (500 ppm); B) *operando* FTIR spectra during TPR. Spectra collected at a) 40 °C; b) 88 °C; c) 130 °C; d) 173 °C; e) 248 °C; f) 300 °C; g) 400 °C. NCO chemigram has been calculated from NCO peaks area (band at 2229 cm^{-1} and 2165 cm^{-1} in panel B).

Fig. 12. A) TPR experiment over Rh-Ba/Al$_2$O$_3$ catalyst from 40 to 400 °C (4 °C/min), with NO (1000 ppm) + CO (1500 ppm) + H$_2$ (500 ppm); B) *operando* FTIR spectra during TPR. Spectra collected at a) 40 °C; b) 70 °C; c) 127 °C; d) 176 °C; e) 218 °C; f) 243 °C; g) 268 °C; h) 318 °C; i) 400 °C. NCO chemigram has been calculated from NCO peaks area (band at 2227 cm^{-1} and 2166 cm^{-1} in panel B).

formed at low temperatures but being readily hydrolysed by water at higher temperatures leading to the formation of ammonia (and CO$_2$) [19,22], that is indeed observed starting from near 200 °C. Accordingly the surface isocyanate concentration rapidly decreases above 200 °C in correspondence with ammonia evolution.

Similar effects are observed in the case of Rh-containing sample, although in this case the effect of water on the onset of the CO/NO reaction is less evident.

3.5. NO/(CO + H$_2$)-TPR

Eventually, the reactivity of NO with CO has also been investigated in the presence of H$_2$, i.e. by using the same reducing mixture used in lean rich cycles. The results are reported in Figs. 11A, 12A (gas phase) and 11B, 12B (surface spectra) , for both Pt-Ba/Al$_2$O$_3$ and Rh-Ba/Al$_2$O$_3$ catalysts, respectively.

In the case of Pt-catalyst, the onset temperature for the consumption of H$_2$/CO is observed near 100 °C, together with evolution of N$_2$O, N$_2$, and CO$_2$ (Fig. 11A). At higher temperature, near 175 °C, ammonia is also detected at the reactor outlet. Complete consumption of NO and H$_2$ is observed near 220 °C, while CO decreases in two steps, being its consumption complete at higher temperature (near 300 °C) where the N$_2$O concentration is nihil.

Fig. 12A reports the gas phase analysis of the TPR experiment carried out over Rh-Ba/Al$_2$O$_3$ catalyst. In this case the onset temperature for gaseous reductants slightly higher than over Pt-catalyst, i.e. near 170 °C, with simultaneous evolution of N$_2$O, N$_2$, and CO$_2$. At higher temperatures, near 225 °C, ammonia is also observed. The complete consumption of NO is observed at slightly higher temperature than over Pt-based system (250 °C vs. 220 °C). Above 300 °C no further evolution
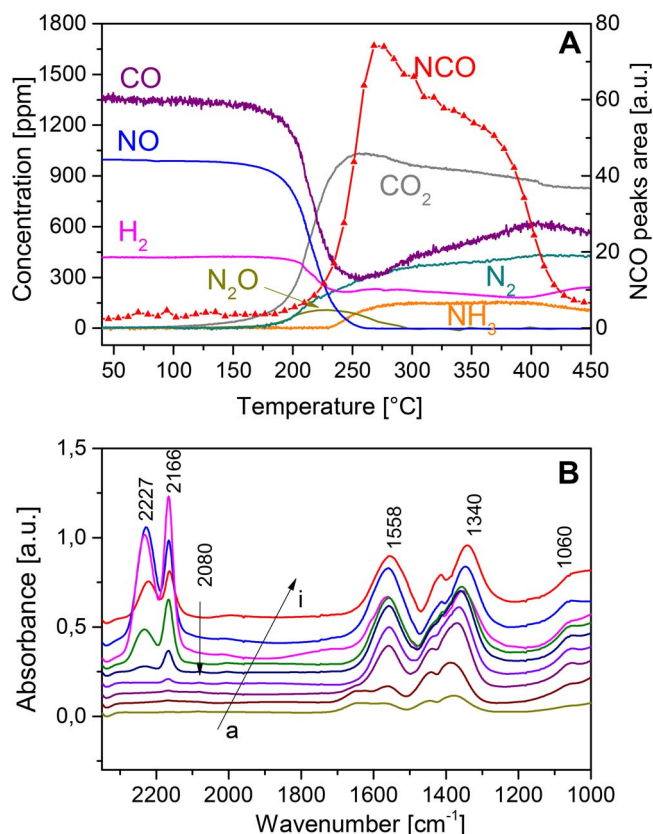
of N$_2$O is observed; both CO and H$_2$ consumption is not complete even at high temperatures.

The surface spectra recorded in this case are shown in Figs. 11B and 12B for Pt-Ba/Al$_2$O$_3$ and Rh-Ba/Al$_2$O$_3$, respectively. Similar features over both catalysts can be observed which closely resemble those previously described in the presence of CO only (see Figs. 6B and 7B). Upon increasing the temperature, several bands develop in the region 1600–1000 cm^{-1} due to carbonates formation on Ba sites. In parallel, bands near 2080 cm^{-1} (shifting towards 2045 cm^{-1} in the case of Pt) grow up corresponding to carbonyls bonded to Pt and Rh sites. At the same time, in the high wavenumbers region, the formation of bands related to isocyanates is observed at ca. 2165 cm^{-1} and 2230 cm^{-1} whose intensity increases monotonically with temperature in the case of Pt-based sample and show a maximum near 300 °C over the Rh-based sample. In both cases, at the end of the heating ramp isocyanates species are still present at the catalyst surface. Of note, over the Rh-based catalyst isocyanates are formed at higher temperature with the respect to the Pt-containing catalyst and their concentration is much lower with respect to the Pt-based catalyst, in line with the data discussed so far.

4. Routes for N$_2$O formation

The results of isothermal lean-rich cycles have clearly shown that N$_2$O is formed both upon the lean/rich (primary N$_2$O) and rich/lean (secondary peak) switches, as already reported in the literature [9,11,29–32]. The primary N$_2$O formation occurs as a peak at the regeneration front, i.e. the early beginning of the regeneration upon reduction of the stored NO$_x$ over partially reduced platinum group metal (PGM) sites [7,9,11]. Primary N$_2$O formation is favored at low temperatures (where the reduction of Pt sites is slower) and is observed with

all reductants [33]. At variance the secondary N_2O peak more strongly depends on the nature of the reductant [33 and references therein].

When using a strong reductant like H_2, the fast reduction of the metal sites results in a sharp N_2O formation peak upon the lean-rich transition since NO released in the gas phase from the stored NO_x species is readily reduced. Also, when no significant amounts of reduced species (like NH_3, isocyanate) are left on the surface after the rich phase, the secondary N_2O peaks is also small. At variance, when CO is co-fed with H_2, higher amounts of N_2O are produced both during the lean/rich and the rich/lean transitions. In fact in the presence of CO the reduction of the metal sites upon the lean/rich transition is slower and this favors the primary N_2O formation. Also, residual reduced species are left onto the surface after the rich phase (i.e. NCO^-, CO ad-species) that could react with NO upon the subsequent NO/O_2 admission giving rise to secondary N_2O formation. In that respect, similar trends have been observed over both Pt- and Rh-based catalyst samples.

The results of TPR/TPSR experiments, coupled with FT-IR analysis of the surface under *operando* conditions, provided further details on the pathways leading to N_2O formation. These experiments clearly illustrated that N_2O formation is favored by the presence of high concentrations of gas-phase NO: in fact significant amounts of N_2O have been observed in the experiments where gas-phase NO is fed to the reactor, whereas no nitrous oxide formation has been observed both over the Pt- and Rh-Ba/Al_2O_3 catalysts upon the reduction of the stored nitrates under temperature programming (TPSR experiments). In fact during these experiments the concentration of gaseous NO released from the adsorbed NO_x is small and N_2O formation according to reactions (5)–(6) is expected to be unlikely. At variance, due to the high reductant/gaseous NO ratio which is attained upon admission of the reductant, NO dissociation to N- and O-adspecies is favored and this prevents N_2O formation [13,28].

Apparently, these findings contrast with results of lean/rich operation, where N_2O formation has been instead observed upon reduction of the stored NO_x. This is due to the different operating conditions: indeed, upon the lean to rich transition, a significant NO release in the gas phase is observed upon reductant admission. This leads to significant NO concentration in the gas phase that in turn favors N_2O formation.

Accordingly, the pathway for N_2O formation upon reduction of the stored NO_x species (rich phase) can be depicted as follows. The reaction is initiated by the reduction of the PGM sites by the reducing agent. This leads to the reduction of the stored NO_x species leading to the release of NO in the gas phase [1,34–36]. The released gaseous NO is dissociated into N- and O-adatoms over reduced Pt and Rh sites (reaction (5)); in case no complete NO dissociation is attained (poorly reduced noble metal sites), N-adsorbed species interact with undissociated NO molecules (either in the gas-phase or from an adsorbed state) leading to the formation of N_2O (reaction (6)):

$$NO + 2\,Me \rightarrow Me\text{-}N + Me\text{-}O \tag{5}$$

$$NO + Me\text{-}N \rightarrow N_2O + Me \tag{6}$$

where Me is the metal site (Pt or Rh) [13,37,38]. Simultaneously, the formed Me-O sites are reduced by the reductant (reaction (19)):

$$Me\text{-}O + 2\,Me\text{-}H \rightarrow 3\,Me + H_2O \tag{19}$$

When the reduction is very efficient (e.g. at high temperatures) NO fully dissociates and the coupling of N-adatoms leads to the formation of N_2, reaction (20):

$$Me\text{-}N + Me\text{-}N \rightarrow N_2 + 2\,Me \tag{20}$$

Accordingly, N_2O formation occurs in the presence of undissociated NO in the gas phase (either already present in the feed stream or released from the stored NO_x) and partially reduced metal sites. When H_2 is used as reductant, N_2O formation occurs at low temperature upon the lean/rich transition and at the beginning of the heating ramp in the TPR runs. N_2O formation is seen at higher temperatures using CO or

$CO + H_2$ mixture, due to the lower reducing capability of these gases.

Besides, isocyanates species may also play a role in N_2O formation. These species are formed during the reduction of NO/stored NO_x in the presence of CO and may originate N_2O upon reaction with NO, as observed in this work during the isocyanate + NO reaction (Fig. 8) and as also pointed in previous studies [29]. These species are also involved in the secondary N_2O emissions, where isocyanates species left on the surface after the rich phase react with NO/O_2 upon the rich/lean transition.

Both the primary and the secondary N_2O formation decrease by increasing the temperature during lean/rich cycles. In fact, at higher temperature the reduction of the metal sites is faster, so that NO dissociation is enhanced thus favoring the coupling of N-adatoms (reaction (20)) with respect to N_2O formation (primary N_2O, reaction (6)). The secondary N_2O formation is also depressed since lower amounts of isocyanates/adsorbed CO are left on the surface at the end of the rich phase [9,31].

Finally, water decreases N_2O formation (when CO is used as reducing agent) in that its presence enhances the reduction of the catalyst (due to H_2 formation via the WGS reaction) and reduces the isocyanates surface concentration as well, being these species readily hydrolyzed to NH_3 and CO_2 [19].

5. Conclusions

In this work mechanistic aspects involved in the formation of N_2O over model Pt-Ba/Al_2O_3 and Rh-Ba/Al_2O_3 LNT catalysts have been discussed. The reactivity of both gaseous NO fed to the reactor and of NO_x (nitrates) stored on the catalyst surface has been studied, with simultaneous surface characterization by *operando* FT-IR spectroscopy, using different reductants (i.e. $CO + H_2$, H_2, CO, $CO + H_2O$) both under isothermal conditions and temperature programming.

During lean/rich cycling operation of the LNT catalysts, N_2O formation may occur during both the lean/rich and rich/lean transitions (primary and secondary N_2O, respectively). Upon the lean to rich switch, N_2O formation is explained on the basis of the slow reduction of the metal sites, that not readily dissociate gaseous NO over the noble metal sites into N- and O-adspecies. Eventually N_2O is formed upon the coupling of undissociated NO with N-adspecies. At variance, N_2O evolution upon the lean to rich transition is due to the reaction with NO/O_2 of reduced species left on the surface at the end of the rich period (e.g. adsorbed CO, isocyanates).

The nature of the reducing agent affects the N_2O formation and accordingly the amounts of the primary and secondary N_2O peak. Using a strong reductant like H_2, the fast reduction of the metal sites results in a small N_2O formation upon the lean-rich transition. Also, no significant amounts of reduced species are left on the surface (e.g. NH_3, isocyanate) during the rich phase, so that the secondary N_2O peaks is also small. On the other hand, the presence of CO favors the formation of both the primary and secondary N_2O in that the rate of reduction of the metal sites is depressed, and residual reducing species (e.g. isocyanates) are left onto the surface after the rich phase.

Both the primary and the secondary N_2O formation decrease by increasing the temperature during lean/rich cycles. In fact, at higher temperature the metal sites are easier reduced by the reducing agent, so that NO dissociation is enhanced. The secondary N_2O formation is also depressed since lower amounts of isocyanates/adsorbed CO are left on the surface at the end of the rich phase.

Water depresses N_2O formation (when CO is used as reducing agent) in that its presence enhances the reduction of the catalyst (due to H_2 formation via the WGS reaction) and reduces the isocyanates surface concentration as well since these species are readily hydrolyzed to NH_3 and CO_2.

Finally, Pt- and Rh-based catalysts have shown similar behavior, but the Rh-containing sample is less reactive than the Pt-based catalyst. This could be partially ascribed to the lower dispersion of Rh with respect to Pt.

References

[1] W.S. Epling, L.E. Campbell, A. Yezerets, N.W. Currier, J.E. Parks, Catal. Rev. Eng. 46 (2) (2004) 163–245.
[2] W.P. Partridge, J.S. Choi, Appl. Catal. B: Environ. 91 (1–2) (2009) 144–151.
[3] J.S. Choi, W.P. Partridge, J.A. Pihl, M.Y. Kim, P. Kočí, C.S. Daw, Catal. Today 184 (1) (2012) 20–26.
[4] L. Masdrag, X. Courtois, F. Can, Daniel Duprez, Appl. Catal. B: Environ. 146 (2014) 12–23.
[5] M.E. Popa, M.K. Vollmer, A. Jordan, W.A. Brand, S.L. Pathirana, M. Rothe, T. Röckmann, Atmos. Chem. Phys. 14 (2014) 2105–2123.
[6] N.W. Cant, D.E. Angove, D.C. Chambers, Appl. Catal. B: Environ. 17 (1998) 63–73.
[7] L. Kubiak, R. Matarrese, L. Castoldi, L. Lietti, M. Daturi, P. Forzatti, Catalysts 6 (2016) 36.
[8] L. Kubiak, L. Righini, L. Castoldi, R. Matarrese, P. Forzatti, L. Lietti, M. Daturi, Top. Catal. 59 (2016) 976–981.
[9] S. Bártová, P. Kočí, D. Mráček, M. Marek, J.A. Pihl, J.S. Choi, T.J. Toops, W.P. Partridge, Catal. Today 231 (2014) 145–154.
[10] P. Dasari, R. Muncrief, M.P. Harold, Top. Catal. 56 (2013) 1922–1936.
[11] P. Kočí, S. Bártová, D. Mráček, M. Marek, J.S. Choi, M.Y. Kim, J.A. Pihl, W.P. Partridge, Top. Catal. 56 (2013) 118–124.
[12] A. Kumar, M.P. Harold, V. Balakotaiah, J. Catal. 270 (2010) 214–223.
[13] J.P. Breen, R. Burch, C. Fontaine-Gautrelet, C. Hardacre, C. Rioche, Appl. Catal. B: Environ. 81 (2008) 150–159.
[14] S. Thomas, O. Marie, P. Bazin, L. Lietti, C.G. Visconti, F. Manenti, M. Daturi, Catal. Today 283 (2017) 176–184.
[15] S. Wuttke, P. Bazin, A. Vimont, C. Serre, Y.K. Seo, Y.K. Hwang, J.S. Chang, G. Férey, M. Daturi, Chem. Eur. J. 18 (38) (2012) 11959–11967.
[16] I. Nova, L. Lietti, L. Castoldi, E. Tronconi, P. Forzatti, J. Catal. 239 (2006) 244–254.
[17] L. Lietti, I. Nova, P. Forzatti, J. Catal. 257 (2008) 270–282.
[18] Y. Ji, T.J. Toops, M. Crocker, Appl. Catal. B: Environ. 140–141 (2013) 265–275.
[19] N. Bion, J. Saussey, M. Haneda, M. Daturi, J. Catal. 217 (2003) 47–58.
[20] T. Lesage, C. Verrier, P. Bazin, J. Saussey, M. Daturi, Phys. Chem. Chem. Phys. 5 (2003) 4435–4440.
[21] P. Forzatti, L. Lietti, I. Nova, S. Morandi, F. Prinetto, G. Ghiotti, J. Catal. 274 (2) (2010) 163–175.
[22] Y. Ji, T.J. Toops, M. Crocker, Appl. Catal. B: Environ. 140–141 (2013) 265–275.
[23] R.D. Clayton, M.P. Harold, V. Balakotaiah, C.Z. Wan, Appl. Catal. B: Environ. 90 (2009) 662–676.
[24] K.I. Hadjiivanov, G.N. Vayssilov, Adv. Catal. 47 (2002) 307–511.
[25] R.G. Greenler, K.D. Burch, K. Kretzchmar, R. Klauser, A.M. Bradshaw, B.E. Hayden, Surf. Sci. 152 (1985) 338.
[26] T. Lesage, C. Verrier, P. Bazin, J. Saussey, S. Malo, C. Hedouin, G. Blanchard, M. Daturi, Top. Catal. 30/31 (2004) 31–36.
[27] S. Morandi, F. Prinetto, G. Ghiotti, L. Castoldi, L. Lietti, P. Forzatti, M. Daturi, V. Blasin-Aubé, Catal. Today 231 (2014) 116–124.
[28] L. Lietti, N. Artioli, L. Righini, L. Castoldi, P. Forzatti, Ind. Eng. Chem. Res. 51 (2012) 7597–7605.
[29] Y. Ji, T.J. Toops, M. Crocker, Appl. Catal. B: Environ. 140–141 (2013) 265–275.
[30] R.D. Clayton, M.P. Harold, V. Balakotaiah, AIChE J. 55 (2009) 687–700.
[31] U. Elizundia, D. Duraiswami, B. Pereda-Ayo, R. López-Fonseca, J.R. González-Velasco, Catal. Today 176 (2011) 324–327.
[32] B. Pereda-Ayo, D. Duraiswami, J.A. González-Marcos, J.R. González-Velasco, Chem. Eng. J. 169 (2011) 58–67.
[33] M. Jabłońska, R. Palkovits, Catal. Sci. Technol. 6 (2016) 7671–7687.
[34] L. Castoldi, L. Righini, R. Matarrese, L. Lietti, P. Forzatti, J. Catal. 328 (2015) 270–279.
[35] K.S. Kabin, R.L. Muncrief, M.P. Harold, Catal. Today 96 (2004) 79–89.
[36] R.L. Muncrief, K.S. Kabin, M.P. Harold, AIChE J. 50 (2004) 2526–2540.
[37] R. Burch, A.A. Shestov, J.A. Sullivan, J. Catal. 188 (1999) 69.
[38] N.W. Cant, D.C. Chambers, I.O.Y. Liu, J. Catal. 278 (2011) 162.